Modeling a Stratocumulus-Topped PBL: Intercomparison among Different One-Dimensional Codes and with Large Eddy Simulation

P. Bechtold,* S. K. Krueger,+ W. S. Lewellen,# E. van Meijgaard,@ C.-H. Moeng,& D. A. Randall,** A. van Ulden,@ and S. Wang++

ABSTRACT

Several one-dimensional (1D) cloud/turbulence ensemble modeling results of an idealized nighttime marine stratocumulus case are compared to large eddy simulation (LES). This type of model intercomparison was one of the objects of the first Global Energy and Water Cycle Experiment Cloud System Study boundary layer modeling workshop held at the National Center for Atmospheric Research on 16–18 August 1994.

Presented are results obtained with different 1D models, ranging from bulk models (including only one or two vertical layers) to various types (first order to third order) of multilayer turbulence closure models. The 1D results fall within the scatter of the LES results. It is shown that 1D models can reasonably represent the main features (cloud water content, cloud fraction, and some turbulence statistics) of a well-mixed stratocumulus-topped boundary layer.

Also addressed is the question of what model complexity is necessary and can be afforded for a reasonable representation of stratocumulus clouds in mesoscale or global-scale operational models. Bulk models seem to be more appropriate for climate studies, whereas a multilayer turbulence scheme is best suited in mesoscale models having at least 100- to 200-m vertical resolution inside the boundary layer.

1. Introduction

The first Global Energy and Water Cycle Experiment (GEWEX) Cloud System Study (GCSS) workshop on boundary layer cloud modeling was held at the National Center for Atmospheric Research on 16–18 August 1994. Two of the main objectives of the GEWEX program are (i) to validate existing cloud parameterization schemes for use in general circulation models (GCMs) and (ii) to develop new parameterization schemes based on numerical data generated from large eddy simulations (LESs) or cloud resolving models (CRMs) (Browning 1993). While 3D LESs can explicitly resolve most of the turbulent eddies, CRMs, which resolve only large cloud elements, are generally utilized for studies on larger domains using lower horizontal resolutions and, therefore, require more sophisticated subgrid turbulence parameterization. To have a high degree of confidence in data generated from LESs or CRMs, we have to validate these models against each other or against observations.

The long-term strategy of the boundary layer working group of GCSS is to gradually model all the different types of cloud-topped boundary layers (stratocumulus, shallow cumulus, cloudiness transition). The first workshop focused on a simple idealized stratocumulus-topped boundary layer. Ten LES and four 2D CRM groups, as well as six one-dimensional (1D) cloud modeling groups, participated in this workshop. Moeng et al. (1996) report the setup of the intercomparison experiment, present an intercompari-

*Laboratoire d'Aérologie, Observatoire Midi-Pyrénées, Toulouse, France.
+Department of Meteorology, University of Utah, Salt Lake City, Utah.
#Department of Meteorology, West Virginia University, Morgantown, West Virginia.
@KNMI, De Bilt, the Netherlands.
&NCAR, Boulder, Colorado.
**Department of Meteorology, Colorado State University, Fort Collins, Colorado.
++NASA/MSFC, Huntsville, Alabama.
Corresponding author address: Dr. Peter Bechtold, Laboratoire D'Aerologie, UMR UPS/CNRS 5560, Observatoire Midi-Pyrénées, 31400 Toulouse, France.
E-mail: becp@aero.obs-mip.fr
In final form 25 March 1996.

son of the LES and 2D CRM results, and discuss the uncertainties that exist in these models. In the present paper we focus on the discussion of the 1D results and compare them to those of the LESs. As model results obtained with very different 1D models, ranging from bulk models to higher-order turbulence models, were available at the workshop, we will profit from the intercomparison of the 1D results to discuss the influence of different turbulence schemes and vertical resolutions on the model results.

2. Description of the 1D codes

The six different 1D modeling groups that participated in this intercomparison project are listed in the appendix. A description of the different models, including the number of prognostic model variables as well as the type of the turbulence and fractional cloudiness scheme employed, is given in Table 1. The models further differ by their treatment of radiation, surface fluxes, and numerics. While the latter two points are of minor importance in the present study, the different treatment of longwave radiation in the models might lead to some quantitative differences in the maximum value of liquid water and buoyancy simulated by the models (Moeng et al. 1996).

a. Turbulence

The different models described in Table 1 can be classified into two main groups: multilayer and bulk models. The multilayer turbulence models include the first-order Royal Netherlands Meteorological Institute (KNMI) model using a nonlocal vertical diffusion scheme together with a prescribed shape of the mixing coefficients, the 1.5-order Laboratoire d'Aerologie, Observatoire Midi-Pyrénées (AERO) model using a prognostic equation for the turbulent kinetic energy (TKE), and the quasi-equilibrium second-order West Virginia University (WVU) model using a prognostic equation for the TKE and an additional prognostic equation for the variance in the departure of the humidity from its saturated value. Finally, the University of Utah (UU) third-order turbulence model includes 11 prognostic equations for second-order moments and 24 for third-order moments. An important point in turbulence models is the specification of the turbulent length scales. However, in the present case of a well-mixed boundary layer all current methods employed to compute these length scales give similar results—that is, a length scale profile that increases from a small value near the surface to a large value in the bulk of the boundary layer. The major differences in the length scale computations concern the rate of decrease with height of the length scales in the neighborhood of the inversion.

The bulk model type is represented by the National Aeronautics and Space Administration (NASA) model and the Colorado State University (CSU) model. In both models the turbulent flux in the boundary layer is computed by a mass flux scheme, and the boundary layer height is determined by a prognostic equation. The NASA model includes two vertical lay-

TABLE 1. The 1D codes: scientists and model characteristics.

1D	Scientist	Turbulence	Subgrid condensation	Number of prognostic variables
AERO	Peter Bechtold	1.5 order	turbulence statistics	5
CSU	David Randall	second-order bulk (mass flux)	mass flux + relative humidity	6
KNMI	Erik van Meijgaard, Aad van Ulden	nonlocal K closure	turbulence statistics	4
NASA	Shouping Wang	bulk (mass flux)	mass flux + relative humidity	7
UU	Steven Krueger	third order	turbulence statistics	39
WVU	Steven Lewellen	second order	turbulence statistics	6

ers, one for the cloud layer and one for the subcloud layer, whereas the CSU model only includes one layer. However, in addition to a prognostic equation for the TKE, the CSU model also provides diagnostic equations for the second-order moments that allow it to relax the well-mixed assumption that is generally used in bulk models.

b. Thermodynamics and cloud fraction

The numbers of prognostic variables used in each model, as indicated in Table 1, include not only the mean horizontal wind components and thermodynamics but also the second- and third-order moments. The thermodynamic variables used in the models are generally conservative variables—that is, the liquid potential temperature or moist static energy together with the total water specific humidity.

The multilayer turbulence models compute both grid volume fractional cloudiness and liquid water content diagnostically using a statistical scheme, but different subgrid distribution functions are used by the modeling groups. However, as shown by Bougeault (1981), the influence of the subgrid distribution on the value of the liquid water content and the cloud fraction is weak in high cloudiness regimes such as stratocumulus clouds where the subgrid distribution is quasi-Gaussian (Cuijpers and Bechtold 1995).

In the bulk models the cloud cover (horizontal grid fraction) is computed as the sum of the updraft fraction, determined from the mass flux scheme, plus an additional term depending on relative humidity. In the NASA model both liquid water content and cloud fraction are predicted by prognostic equations.

3. An idealized nighttime stratocumulus case

For simplicity we chose an idealized nighttime marine stratocumulus case with low surface heating and little wind shear. Furthermore, solar radiation and drizzle were excluded in this experiment. Therefore, the turbulence in the planetary boundary layer was mainly driven by longwave cooling at the cloud top, water loading, and diabatic heating through condensation/evaporation.

A detailed description of the experiment and the numerical setup has already been presented by Moeng et al. (1996). The initial sounding is loosely based on the FIRE [First ISCCP (International Satellite Cloud Climatology Project) Regional Experiment] solid stratocumulus sounding reported in Betts and Boers (1990). However, the original sounding was changed to nighttime, which had significantly lower wind speed [please refer to Moeng et al. (1996) for a description of the FORTRAN code used to generate the sounding]. The sea surface temperature is 288 K. The dry potential temperature profile is slightly stable in the PBL and increases from 288 K at the surface to 288.32 K at the inversion base at 690 m, and then rapidly increases to a value of 294.4 K at the inversion top at 785 m. The cloud layer itself is initially unstable. The total water mixing ratio (water vapor plus liquid water) is constant in the PBL, with a value of 8.1 g kg^{-1}, and decreases to a value of 4.6 g kg^{-1} throughout the inversion. The surface mixing ratio is set equal to the saturation mixing ratio. Finally, the horizontal wind components u and v have constant values of 2 and -4 m s^{-1}, respectively, throughout the whole numerical domain and are equal to the respective geostrophic components. An overview of the numerical setup of the 1D simulations is given in Table 2. Note that the vertical resolution used in the multilayer models vary from a uniform grid to a varying grid with finer resolution in the neighborhood of the inversion.

4. Intercomparison results

a. Time evolution

In Fig. 1 we present the time evolution of the cloud-top height, the cloud cover, the vertically integrated liquid water path, and the PBL-averaged TKE and

TABLE 2. One-dimensional simulation parameters.

Sea surface temperature	288 K
Surface pressure	1000 hPa
Large-scale divergence	5×10^{-6} s^{-1}
Coriolis parameter	10^{-4} s^{-1}
Air density	1 kg m^{-3}
Roughness length	2×10^{-4} m
Vertical grid space	25 m
Simulation time	2 hours

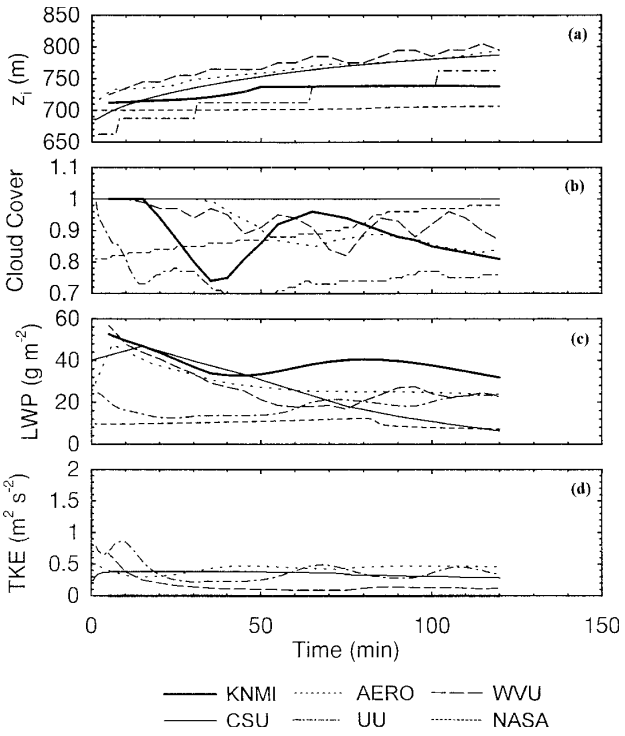

FIG. 1. Time evolution of (a) cloud-top height, (b) fractional cloud cover, (c) vertically integrated liquid water path, and (d) boundary layer averaged TKE from the six different 1D simulations: thick solid line for KNMI, thin solid line for CSU, dotted line for AERO, dashed–dotted line for UU, long-dashed line for WVU, and short-dashed line for NASA.

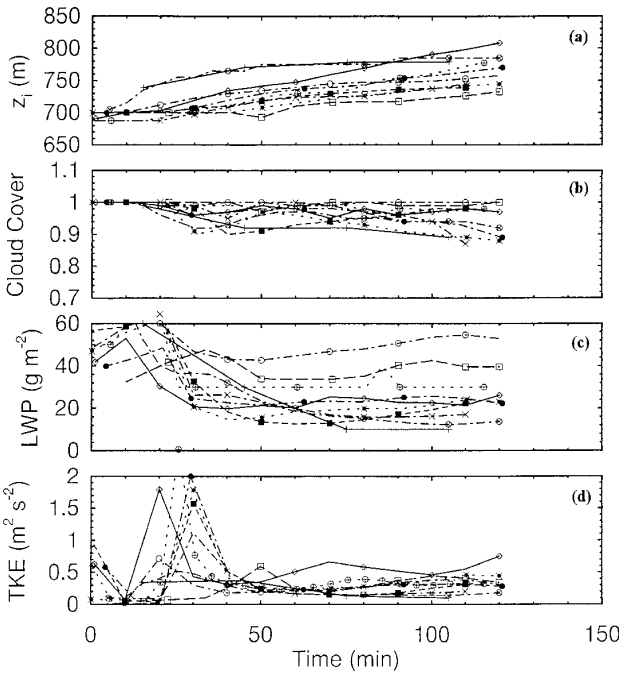

FIG. 2. Same as in Fig. 1 but for different LES simulations.

compare these values to the corresponding 3D LES results in Fig. 2. The LES results represent horizontal averages over a 3.5 km × 3.5 km domain. Concerning the fractional cloud cover, in 1D it is defined as the maximum of the fractional cloud amounts of all levels, whereas in the LES it is defined as the fraction of grid columns that have cloud water. From Fig. 1 we see that the 1D models produce a boundary layer top that rises from 700 m to about 750–800 m at the end of the simulation. Note that the time variation of the PBL top is directly proportional to the entrainment rate as it is given by the difference between the entrainment velocity and the prescribed large-scale subsidence. The final values for the cloud cover vary between 70% and 100%, with the multilayer models producing less than 100% cloud cover and the CSU bulk model producing 100% cover. The integrated liquid water path varies between 10 and 40 g m^{-2}, and here again the values produced by the multilayer models are very close. Finally, the PBL-averaged TKE (only for the models having a prognostic equation for TKE) attains a final stationary value varying between 0.2 and 0.5 m^2 s^{-2}.

Comparing these results to the corresponding LES results in Fig. 2, we observe that the spread in the 1D results is comparable to that in the LES after the adjustment time of roughly 1 hour. As mentioned by Moeng et al. (1996), one reason for the spread in the LES results is that different radiation codes produce substantially different radiative cooling rates and consequently different values of TKE and entrainment. The higher-order turbulence model and the CSU bulk model show an average entrainment rate of 0.9 cm s^{-1} over the second hour of simulation, which corresponds reasonably to the average LES value. However, in contrast to the LES results, the 1D results did not allow the establishment here of a linear relationship between the entrainment velocity and the TKE. One interesting point of this comparison is that concerning the TKE evolution, the 1D models show a better agreement with the 3D LESs than the 2D CRMs, which produced values of about 0.9 m^2 s^{-2} (see Fig. 10 in Moeng et al. 1996). Indeed, the 2D CRMs produced too-high values of TKE because the large eddies in these models are 2D and transport properties vertically less efficiently per unit of turbulent kinetic energy than 3D large eddies. One-dimensional turbulence closure schemes parameterize all turbulent eddies and do not make any assumption about the shape of the turbulent eddies.

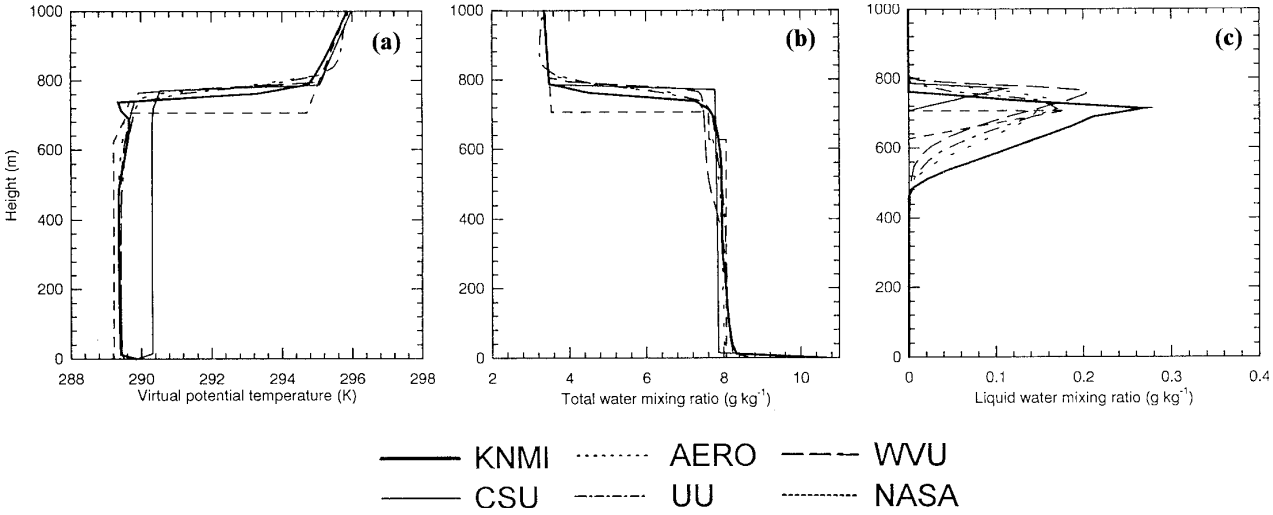

FIG. 3. Vertical profiles of (a) virtual potential temperature, (b) total water mixing ratio, and (c) liquid water mixing ratio for simulation hour 1.5 from the six 1D codes.

b. Vertical profiles

The following vertical profiles are snapshots at simulation hour 1.5 in the 1D models, while the corresponding LES profiles represent time averages over hour 1 to 2. Figure 3 illustrates the vertical profiles of the virtual potential temperature, the total water mixing ratio, and the liquid water content. All 1D models produce quite similar results: a well-mixed PBL and a maximum liquid water mixing ratio ranging from 0.15 to 0.3 g kg^{-1}, with a maximum value of 0.3 g kg^{-1} from the KNMI model. A slightly decoupled boundary layer structure was produced by the WVU model. The 1D results fit within the scatter of the corresponding LES profiles shown in Fig. 4. Some LESs produced a larger maximum liquid water content of up to 0.3 g kg^{-1} and a slightly decoupled boundary layer structure. As discussed in Moeng et al. (1996), the larger liquid water content is due to larger radiative forcing, whereas the decoupled boundary layer structure indicates that the corresponding LES simulation has not reached its final stationary state. However, we do not retrieve this feature in the 1D models where the maximum radiative cooling rate is produced by the WVU model (using higher vertical resolution near cloud top), with a value of 6 K h^{-1} in contrast to a value of 2 K h^{-1} in the CSU model and roughly 4 K h^{-1} in the other models (Fig. 5).

Next, in Figs. 6 and 7 we compare the 1D simulated profiles of the total momentum flux, the buoyancy flux, and the total water flux to the corresponding LES values. As expected, the profiles of the second-order moments show a much larger variability between different models for 1D and LES than the profiles of the first-order moments. Given this vari-

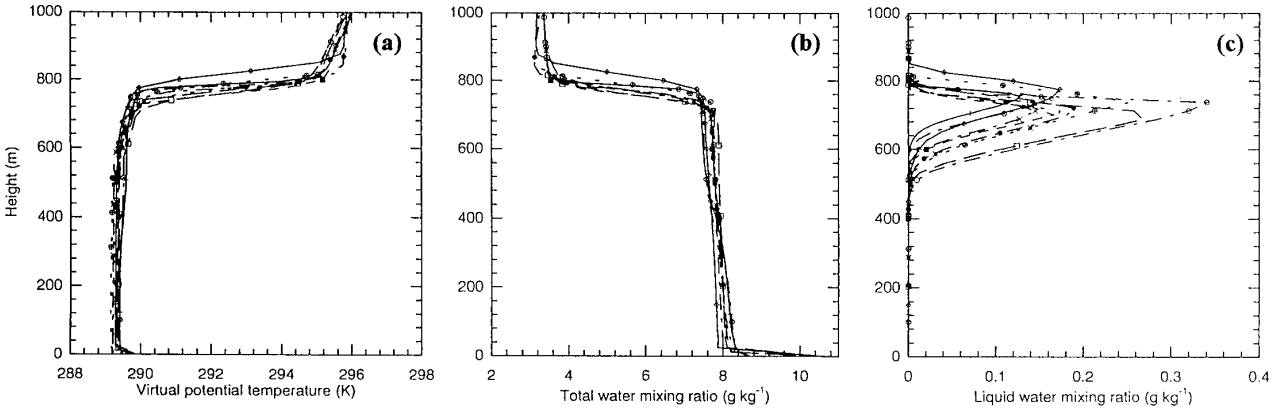

FIG. 4. Same as in Fig. 3 but from different LESs averaged over the second hour of simulation.

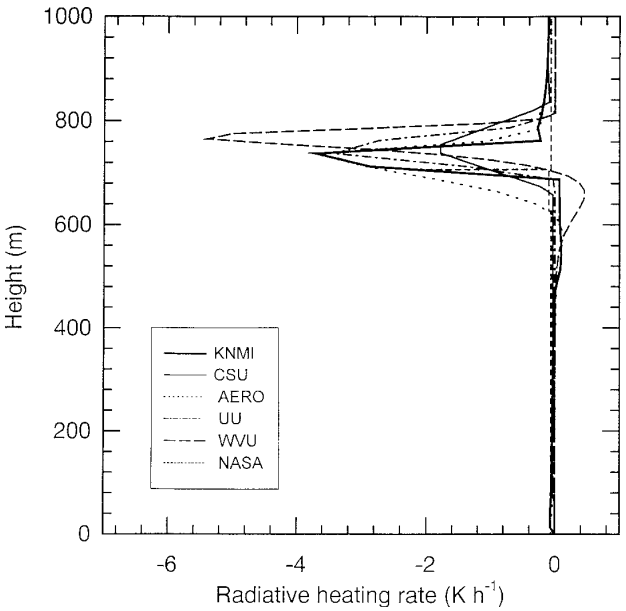

FIG. 5. Same as in Fig. 3 but for the radiative cooling rates (K h^{-1}).

ability, it is difficult to intercompare the 1D and the LES. Nevertheless, all 1D models produced the two main features, which are a maximum buoyancy flux in the cloud layer and a quasi-linear total water flux profile. The fluxes of conserved variables are expected to be approximately linear between surface values and cloud-top values that are determined by entrainment and radiative flux divergence. The lowest flux values (we only consider here the maximum values) are produced by the NASA model and the highest ones by the WVU model, with a maximum flux difference attaining 30 W m^{-2} for the buoyancy flux and 60 W m^{-2} for the total water flux. There is no clear correlation between the buoyancy flux produced by the models and the amount of radiative heating. Therefore, the differences in the buoyancy flux seem to be mainly due to differences in the treatment of turbulence. Concerning the momentum fluxes, we observe too-large values in the AERO model.

Finally, we illustrate the TKE profiles in Fig. 8. Only the 1D having a prognostic equation for TKE could provide profiles. The LESs show a maximum value of TKE below the cloud top. This feature is also reproduced by the AERO model and the WVU model (not shown), whereas the UU model produced a TKE profile that is nearly constant with height.

The intercomparison of the 1D modeling with LES can be summarized as follows. When evaluating the above intercomparison, we have to take into account that 1D models cannot explicitly represent cloud-top entrainment through engulfment of upper-layer warm and dry air (e.g., Breidenthal and Baker 1985; Moeng et al. 1995). Furthermore, 1D cloud/turbulence ensemble models have closure problems, especially on the turbulent length scales in multilayer schemes or the entrainment rates in mass flux schemes. One-dimensional model versions should be considered as tools for comparing the subgrid parameterization to be used in mesoscale or global-scale 3D operational models. In view of these remarks we can say that present 1D cloud/turbulence ensemble models can reasonably represent the evolution of a well-mixed stratocumulus-topped PBL.

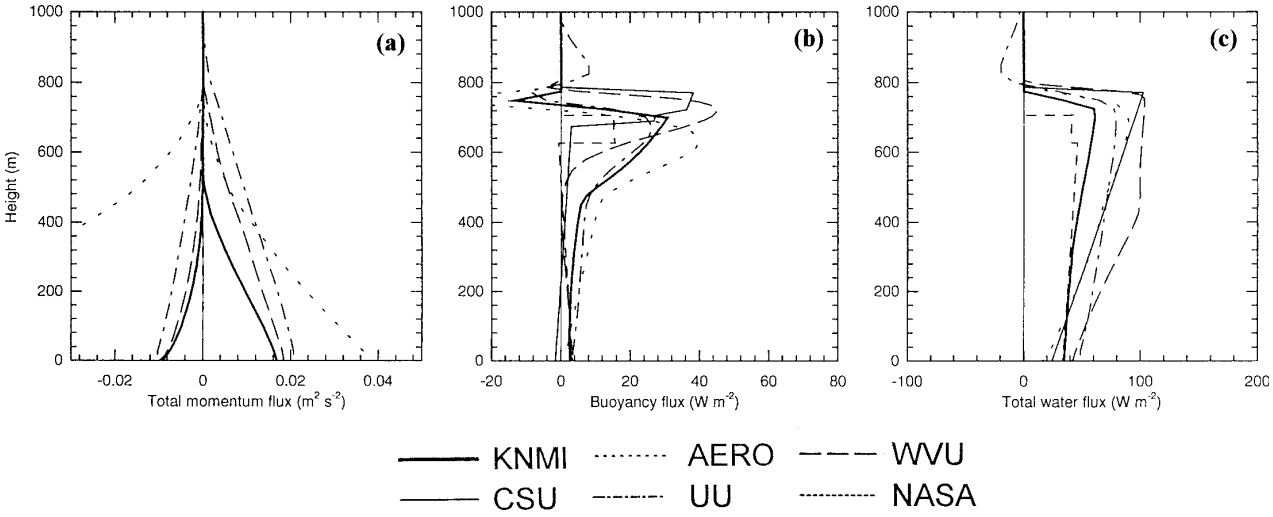

FIG. 6. Vertical profiles of (a) momentum fluxes of *u* and *v*, (b) buoyancy flux, and (c) total water flux at simulation hour 1.5 from the six 1D codes.

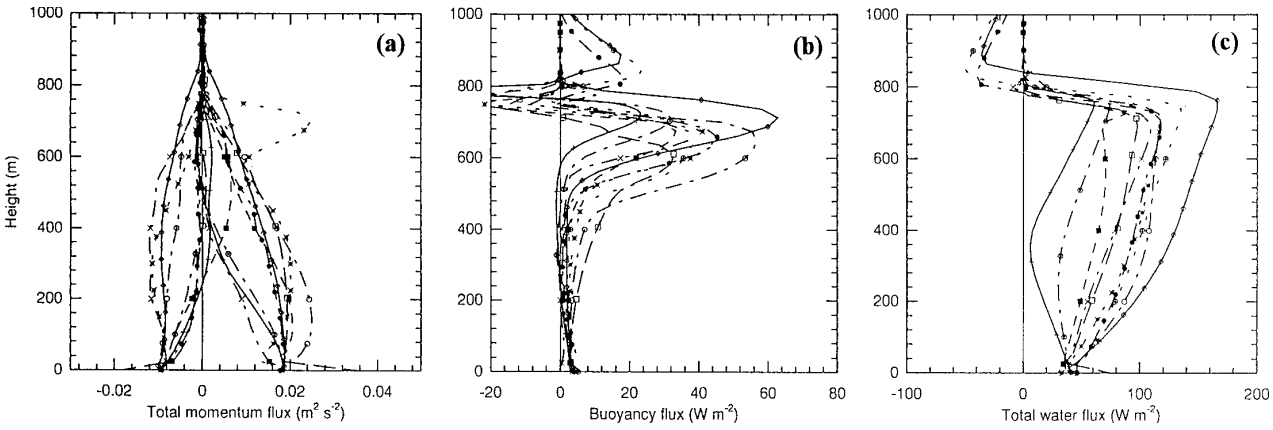

FIG. 7. Same as in Fig. 6 but from different LES averaged over the second hour of simulation.

5. Sensitivity to vertical resolution

In the present idealized stratocumulus experiment we demonstrated that high-resolution 1D turbulence models can produce results that are comparable to LES results. However, in present operational forecast models the vertical resolution in the PBL is at most 100 or 200 m, whereas in present climate models the number of vertical layers in the PBL typically ranges between one and four. Therefore, it is desirable to test the 1D multilayer models at resolutions comparable to that used in operational models.

Four sensitivity tests have been run on the present stratocumulus case using vertical resolutions of 25, 50, 100, and 200 m. The actual thickness of the stratocumulus layer was about 300 m, so that this sensitivity design corresponds to 12, 6, 3, and 1 model layers, respectively, inside the cloud layer. The model runs have been done with the AERO model, which is used here as a representative for all the multilayer models. Figure 9 illustrates the time evolution of the cloud-top height and the cloud cover for the four different runs, and Fig. 10 illustrates the vertical profiles of cloud water and TKE at simulation hour 1.5. We observe that the results obtained with 25- and 50-m resolutions are nearly identical, and to a lesser degree the result with a 100-m vertical resolution is still quite reasonable, although no growth in boundary layer height is seen over the 2-hour simulation in this case. However, the model accuracy decreases quickly when the vertical resolution goes down to 200 m; in particular, the modeled cloud cover of 60% is much too low.

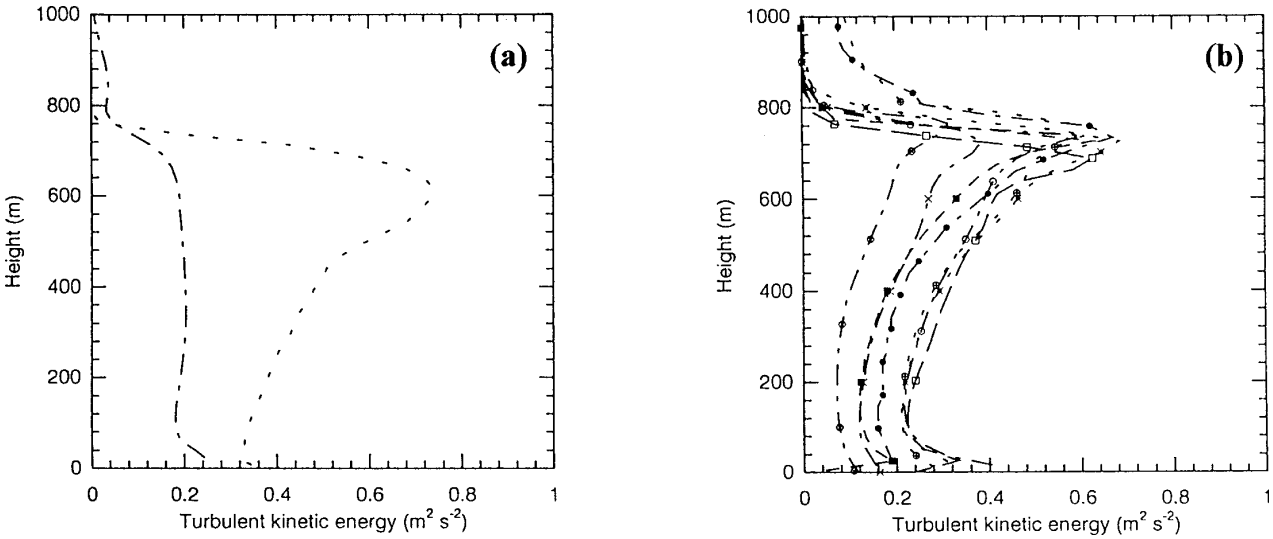

FIG. 8. Vertical profiles of the TKE from (a) the 1D codes and (b) the LESs.

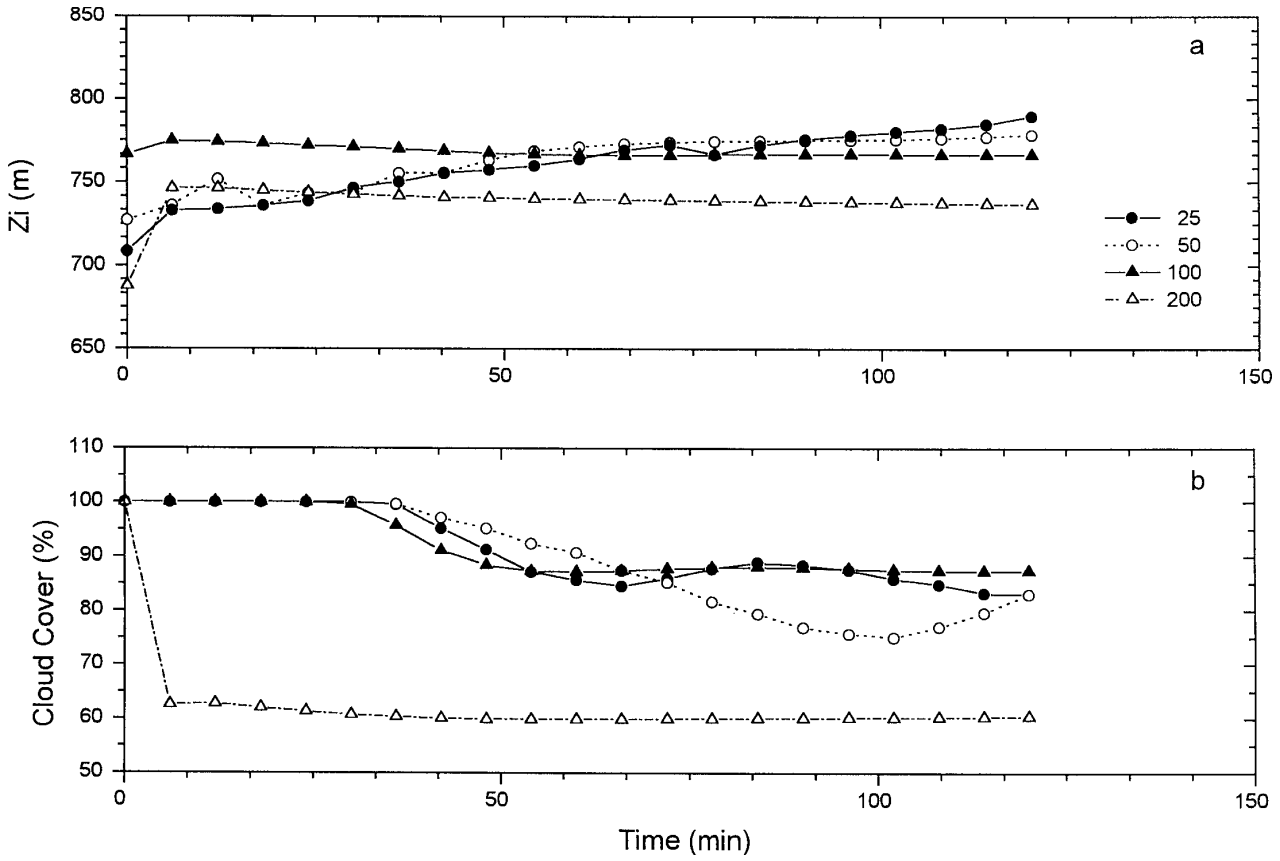

FIG. 9. Time evolution of (a) cloud-top height and (b) cloud cover from four simulations with different vertical resolutions from the 1D AERO model.

We conclude that in multilayer turbulence models a minimum number of vertical levels inside the cloud layer is necessary (typically three) to crudely estimate the cloud-layer dynamics. Vertical resolutions of 100 m still produce quite reasonable results in spite of the fact that in nature radiative cooling at cloud top occurs in a layer of just a few meters. Furthermore, when comparing the results obtained with 200-m vertical resolution to those obtained with the bulk model type (Figs. 1 and 3), we see that a bulk model might produce results that are superior to those of a multilayer turbulence model. By virtue of its formulation, the bulk model is less sensitive to the vertical resolution than the multilayer model.

6. Summary and conclusions

We discussed 1D cloud (turbulence) ensemble model results for an idealized nighttime marine stratocumulus case, as defined by the GCSS boundary layer working group, and compared them to data generated from several 3D LESs. Most of the 1D results (apart from the two bulk models) and the LES results were obtained with the same vertical resolution of 25 m. The six different 1D models presented in this intercomparison study included three higher-order turbulence models, all having one prognostic equation for the TKE (one 1.5-order model, one quasi-equilibrium

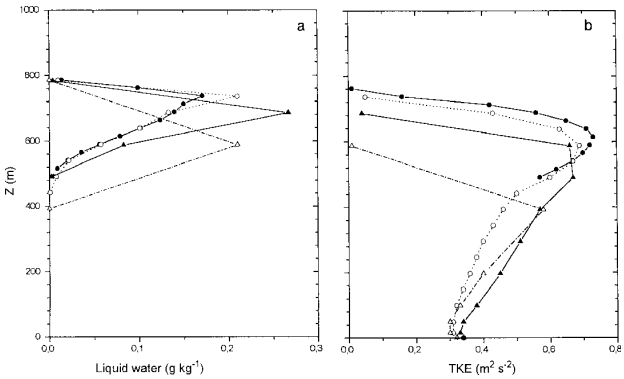

FIG. 10. Same as in Fig. 9 but for the vertical profiles of (a) liquid water content and (b) TKE at simulation hour 1.5.

second-order model, and one third-order model) as well as one nonlocal K-closure model and two bulk models. In contrast to the multilayer models, the bulk models include only one or two vertical layers.

Comparing the 1D and LES results, we noticed that the results obtained with the different multilayer turbulence schemes are very close to each other and fall within the scatter of the LES results. The TKE predicted from the higher-order turbulence models has a closer agreement with that from the LESs than that from the 2D CRMs. Of course, given their nature, the bulk models could not reproduce the detailed vertical structure of the cloud-topped boundary layer; nevertheless, they are able to reproduce a reasonable PBL structure.

An important issue for the GCSS boundary layer working group is to develop or to determine a scheme that best and most efficiently represents the cloudiness, as well as the associated turbulent or convective transport, in the boundary layer. What we compared here were complete models rather than turbulence schemes only. The surface fluxes in the present study were small so that the main sources of difference between the models are due to their vertical structure, the treatment of turbulence and convection, and the radiation scheme used. Furthermore, when addressing the above issue we should be careful, as some models, especially the two bulk models, are still in the developmental stage. Nevertheless, some conclusions on this issue can be put forward. It is evident that a bulk model cannot represent the detailed structure of the PBL as a multilayer model. However, the bulk model is numerically efficient and is a well-adapted tool for climate studies where low vertical model resolutions are necessary. As shown in our sensitivity study, the multilayer turbulence schemes require at least about three model layers in the cloud layer to crudely represent cloud-layer dynamics. At low vertical resolutions, 200 m in the present study, the multilayer models performed worse than the bulk models. Present mesoscale numerical models and possibly future general circulation models might afford 100- to 200-m vertical resolution in the PBL, which indicates that the choice between bulk or multilayer turbulence schemes is still not settled. At equal accuracy we should prefer the most simple turbulence scheme. The present stratocumulus study suggests that a model including a nonlocal first-order or 1.5-order turbulence scheme can be as adapted to the modeling of a well-mixed stratocumulus-topped PBL as a scheme including additional prognostic or diagnostic equations for other second-order or third-order moments. But this conclusion might not be valid when simulating a trade wind cumulus boundary layer where higher-order turbulent moments may be important, and therefore a higher-order turbulence scheme or a shallow convection mass flux scheme might be better adapted.

In the future the GCSS boundary layer working group will concentrate on an idealized entrainment experiment consisting of a smoke cloud layer (with zero surface fluxes, zero evaporational cooling/heating, and a specified radiation flux algorithm), in order to examine in detail cloud-top entrainment as simulated by LES and modeled with the aid of 1D turbulence parameterizations. Furthermore, we will use the Atlantic Stratocumulus Transition Experiment dataset described in Bretherton and Pincus (1995) and Bretherton et al. (1995) to investigate the usefulness of 1D models in simulating a trade wind cumulus boundary layer and a stratocumulus-to-cumulus transition.

Acknowledgments. We would like to express our gratitude to Dr. W. R. Cotton, who leads the GCSS Boundary-Layer Cloud Working Group. This research was partially supported by grants from PATOM (INSU/CNRS France) and by Office of Naval Research Grant N00014-91-J-1175.

Appendix: 1D modeling groups abbreviations and references

AERO	Laboratoire d'Aérologie UMR UPS/CNRS 5560, Observatoire Midi-Pyrénées, Toulouse, France	Bechtold et al. (1992, 1995), Cuijpers and Bechtold (1995)
CSU	Colorado State University, Fort Collins, Colorado	Randall et al. (1992)
KNMI	Royal Netherlands Meteorological Institute, De Bilt, the Netherlands	Holtslag and Boville (1993), Holtslag et al. (1995)
NASA	Universities Space Research Association, NASA/MSFC, Huntsville, Alabama	Albrecht et al. (1979), Wang (1993, 1996)
UU	University of Utah, Salt Lake City, Utah	Krueger (1988)
WVU	West Virginia University, Morgantown, West Virginia	Oliver et al. (1978), Lewellen and Lewellen (1996)

References

Albrecht, B. A., A. K. Betts, W. H. Schubert, and S. K. Cox, 1979: A model of the thermodynamic structure of the trade-wind boundary layer. Part I: Theoretical development and sensitivity tests. *J. Atmos. Sci.,* **36,** 73–89.

Bechtold, P., C. Fravalo, and J.-P. Pinty, 1992: A model of marine boundary layer cloudiness for mesoscale applications. *J. Atmos. Sci.,* **49,** 1723–1744.

——, J. W. M. Cuijpers, P. Mascart, and P. Trouilhet, 1995: Modeling of trade wind cumulus clouds with a low-order turbulence model: Toward a unified description of Cu and Sc clouds in meteorological models. *J. Atmos. Sci.,* **52,** 455–463.

Bougeault, P., 1981: Modeling the trade-wind cumulus boundary layer. Part I: Testing the ensemble cloud relations against numerical data. *J. Atmos. Sci.,* **38,** 2414–2428.

Breidenthal, R. E., and M. B. Baker, 1985: Convection and entrainment across stratified interfaces. *J. Geophys. Res.,* **90,** 13 055–13 062.

Bretherton, C. S., and R. Pincus, 1995: Cloudiness and marine boundary layer dynamics in the ASTEX Lagrangian experiments. Part I: Synoptic setting and vertical structure. *J. Atmos. Sci.,* **52,** 2707–2723.

——, P. Austin, and S. T. Siems, 1995: Cloudiness and marine boundary layer dynamics in the ASTEX Lagrangian experiments. Part II: Cloudiness, drizzle, surface fluxes, and entrainment. *J. Atmos. Sci.,* **52,** 2724–2735.

Browning, K. A., 1993: The GEWEX Cloud System Study (GCSS). *Bull. Amer. Meteor. Soc.,* **74,** 387–399.

Cuijpers, J. W. M., and P. Bechtold, 1995: A simple parameterization of cloud water related variables for use in boundary layer models. *J. Atmos. Sci.,* **52,** 2486–2490.

Holtslag, A. A. M., and B. A. Boville, 1993: Local versus nonlocal boundary layer diffusion in a global climate model. *J. Climate,* **6,** 1825–1842.

——, E. van Meijgaard, and W. C. de Rooy, 1996: A comparison of boundary layer diffusion schemes in unstable conditions over land. *Bound.-Layer Meteor.,* in press.

Krueger, S. K., 1988: Numerical simulation of tropical cumulus clouds and their interaction with the subcloud layer. *J. Atmos. Sci.,* **45,** 2221–2250.

Lewellen, D. C., and W. S. Lewellen, 1996: Influence of Bowen ratio on boundary layer cloud structure. *J. Atmos. Sci.,* **53,** 175–187.

Moeng, C.-H., D. Lenschow, and D. A. Randall, 1995: Numerical investigations of the roles of radiative and evaporative feedbacks in stratocumulus entrainment and breakup. *J. Atmos. Sci.,* **52,** 2870–2883.

——, and Coauthors, 1996: Simulation of a stratocumulus-topped planetary boundary layer: Intercomparison among different numerical codes. *Bull. Amer. Meteor. Soc.,* **77,** 261–278.

Oliver, D. A., W. S. Lewellen, and G. G. Williamson, 1978: The interaction between turbulent and radiative transport in the development of fog and low-level stratus. *J. Atmos. Sci.,* **35,** 301–316.

Randall, D. A., Q. Shao, and C.-H. Moeng, 1992: A second-order bulk boundary layer model. *J. Atmos. Sci.,* **49,** 1903–1923.

Wang, S., 1993: Modeling marine boundary layer clouds with a two-layer model: A one-dimensional simulation. *J. Atmos. Sci.,* **50,** 4001–4021.

——, 1996: Defining marine boundary layer clouds with a prognostic scheme. *Mon. Wea. Rev.,* **124,** 1817–1833.